Sphk1-induced Autophagy in Microglia Promotes Neuronal Injury Following Cerebral Ischemia-Reperfusion

Manhua Lv (lvmanhua7266@163.com)
First Affiliated Hospital of Harbin Medical University
Yongjia Jiang
First Affiliated Hospital of Harbin Medical University
Dayong Zhang
Harbin Institute of Technology
Dan Yao
First Affliated Hospital of Harbin Medcial University
Yuefeng Cheng
First Affiliated Hospital of Harbin Medical University
Wei Zhang
First Affiliated Hospital of Harbin Medical University
Yuanyuan Zeng
First Affiliated Hospital of Harbin Medical University

Research

Keywords: cerebral ischemia reperfusion, microglia, Sphingosine Kinase 1, Sphingosine-1-phosphate, autophagy, neuroinflammation

Posted Date: October 15th, 2020

DOI: https://doi.org/10.21203/rs.3.rs-91557/v1

Abstract

Background: Microglial hyperactivation driven by SphK1/S1P signaling and consequent inflammatory mediator production is a key driver of cerebral ischemia-reperfusion injury (CIRI). While SphK1 reportedly controls autophagy and microglial activation, it remains uncertain as to whether it is similarly able to regulate damage mediated by CIRI-activated microglia.

Methods: In the present study, we utilized both an *in vitro* oxygen-glucose deprivation reperfusion (OGDR) model and an *in vivo* rat model of focal CIRI to test whether Sphk1 and autophagy is expressed in microglia. Western blot analysis was used to estimate the autophagy protein level (LC3 and SQSTM) at different time points after OGDR. To detect cytokine secretion in microglial supernatants in response to OGDR, we measured the concentration of IL-1β, IL-6 and TNF-α in the culture supernatants using an enzyme-linked immunosorbent assay (ELISA). To evaluate whether microglia subjected to OGDR exhibited neuronal injury, we used a commercially available terminal transferase-mediated deoxyuridine triphosphate-biotin nick end labeling (TUNEL) kit and flow cytometry to detect apoptotic neurons.

Results: We determined that in the context of CIRI, microglia upregulated SphK1 and induced autophagy, while inhibiting these changes by lentivirus targeting SphK1 significantly decreased expression of autophagy . Moreover, we determined that autophagic body formation was enhanced in cerebral tissues following I/R. We also explored the impact of SphK1-induced autophagy on microglial inflammatory cytokine production and associated neuronal apoptosis using an *in vitro* OGDR model system. At a mechanistic level, we found that SphK1 promotes autophagy via the tumor necrosis factor receptor-associated factor 2 (TRAF2) pathway.

Conclusion: These results reveal a novel mechanism whereby SphK1-induced autophagy in microglia can contribute to the pathogenesis of CIRI, potentially highlighting novel avenues for future therapeutic intervention in IS patients.

Background

Ischemic stroke (IS) is one of the leading causes of death and disability globally, imposing a significant personal and financial burden on the families of those affected by this condition (1). Cerebral ischemia-reperfusion injury (CIRI) is a common mechanism of pathophysiological damage in IS. CIRI results from multiple interacting mechanisms including excessive oxidative stress (OS), calcium overload, excitatory amino acid toxicity, and inflammation, leading to central nervous system damage (2). It is therefore important that the mechanistic basis for CIRI be better studied in order to understand the best therapeutic approaches to preventing and treating this deleterious damage.

Recent work has highlighted the importance of inflammatory immune responses as drivers of CIRI, with microglia, which are the primary immune cells responsible for inflammation within the central nervous system (CNS), being rapidly activated following cerebral ischemia (3). Microglial hyperactivation can lead these cells to produce high levels of neurotoxic and inflammatory compounds such as nitric oxide (NO),

tumor necrosis factor (TNF-α), interleukin (IL-6), interleukin (IL-1β), and reactive oxygen species (ROS) (4). These cytokines and compounds can directly drive the apoptotic or necrotic death of proximal neurons, and can recruit additional cells including macrophages and γδ T cells to the site of ischemia wherein they can secrete additional neurotoxic and inflammatory factors.

Sphingosine 1-phosphate (S1P) is a sphingolipid that controls cellular proliferation, migration, differentiation, and adhesion. S1P generation is mediated by the rate-limiting enzymes sphingosine kinase 1 (SphK1) and sphingosine kinase 2 (SphK2), which thus control sphingolipid signaling in cells (5–9). Microglia are one of the primary cellular sources of SphK1 activity in the context of cerebral ischemia, and inhibiting this enzyme can reduce microglial pro-inflammatory mediator production in the presence of ischemic neurons (10). We have previously shown that Sphk1/S1P regulate the CIRI-associated production of interleukin-17 (IL17) by activated microglia, which can drive the apoptotic death of neurons (11). SphK1/S1P regulate important processes including autophagy and cell survival (12–14). TRAF2 is a key signaling intermediary that is also necessary for the production of inflammatory cytokines (15–17), leading researchers to explore its relationship with intracellular S1P. In hepatoma cells, SphK1 is also known to signal through tumor necrosis factor receptor-associated factor 2 (TRAF2) and to thereby promote autophagy-mediated CDH1/E-cadherin degradation, ultimately facilitating the epithelial-mesenchymal transition of these cancer cells (18).

Autophagy is an essential process whereby cells are able to remove or recycle damaged or unnecessary organelles and proteins via the formation of lysosome-like autophagosomes. Autophagy is closely linked with microglial inflammation in the context of IS, as impaired autophagic responses are associated with increased stroke-related inflammation and brain injury (19). Yang et al (20) determined that chronic cerebral hypoperfusion was able to drive autophagy and activation within microglia and to lead to increased white matter lesion formation and cognitive deficits in a murine model system, whereas the autophagy inhibitor 3-methyadenine (3-MA) was sufficient to inhibit autophagy within these microglia. A separate study also found that ischemia was associated with microglial autophagy and with resultant inflammation and neuronal damage, with 3-MA significantly reducing this microglia-mediated inflammation (21). As such, these results offer evidence suggesting that inhibiting autophagy can improve outcomes associated with reduced cerebral perfusion.

Previous work has confirmed that the dissemination of gastric cancer can be enhanced by Sphk1-induced autophagy (22). While SphK1 is thus directly associated with autophagy, its specific roles and regulatory functions in microglia in the context of CIRI remain uncertain. In this study, we found that during CIRI the microglial expression of LC3 and the activity of SphK1 were increased, whereas the expression of SQSTM1 was reduced in these same cells. Moreover, we determined that autophagic body formation was enhanced in cerebral tissues following I/R. We also explored the impact of SphK1-induced autophagy on microglial inflammatory cytokine production and associated neuronal apoptosis using an *in vitro* oxygen-glucose deprivation reperfusion (OGDR) model system. At a mechanistic level, we found that TRAF2 regulated SphK1-induced autophagy in these cells, thereby controlling inflammation and associated neuronal apoptosis under OGDR conditions.

Methods

Animals

Male Wistar rats (240–260 g) were obtained from the Experimental Animal Center of the Second Affiliated Hospital of Harbin Medical University, and were housed with free access to food and water in a temperature- and humidity-controlled facility with a 12 h light/dark cycle. Prior to experimental utilization, all animals were given a 1 week acclimatization period. All animal studies were approved by the School of Medical Science of Harbin Medical University, with all efforts having been made to reduce animal use and suffering when possible.

Reagents and antibodies

Rabbit anti-rat MAP1LC3 were purchased from Cell Signaling Technology (USA). Rabbit anti-rat Sphk1 was obtained from NOVUS. Rabbit anti-rat SQSTM1, rabbit anti-rat TRAF2, mouse anti-rat Ibal, and mouse anti-rat Neun were purchased from Abcam (USA). Fluorescently labeled anti-rabbit and anti-mouse IgG were from Invitrogen (USA). A TUNEL staining kit was obtained from Roche (Switzerland). S1P, Rapamycin (RAP), and 3-MA were obtained from Sigma. An siRNA specific for rat TRAF2 was purchased from GenePharma Corporation (Shanghai, China).

Focal cerebral ischemia-reperfusion model

In order to study CIRI *in vivo,* we employed a slightly modified version of the previously described middle cerebral artery occlusion (MCAO) model (Lv et al., 2011). Briefly, 10% chloral hydrate (350 mg/kg) was intraperitoneally injected into rats in order to achieve deep anesthesia, after which the neck was opened such that the common carotid artery (CCA) was visible. The proximal ends of the CCA and the internal CA (ICA) were then clamped, and a small V-shaped incision was made in the external carotid artery (ECA). A bolt of thread was then inserted through this incision for MCAO embolization, with a knot being created at the site of thread entry. The clamp on the CCA was then loosened, with the CCA being adjusted until positioned 45 degrees to the right lateral side. The thread was then inserted further until resistance was detected. Blood flow was disrupted for 2 h, after which the embolic thread was removed to the ECA stump as a means of simulating IRI. Control animals underwent the same surgical manipulation but without thrombus insertion. After completion of all surgical procedures, rats were warmed using heating pads and were individually housed with free access to food and water. Animals were subjected to downstream analyses at 12, 24, and 48-h post-surgery.

Immunohistochemistry

Immunofluorescent staining was used to visualize the microglial expression of Sphk1 (NOVUS Biologicals, JA31-14), MAPLC3 II (Cell Signaling Technology, D11) , SQSTM1/p62 (Abcam, ab155686), and TRAF2 (Abcam, ab126758) in our experimental system. Briefly, we initially used xylene to deparaffinize ischemic penumbra tissue sections from model animals. Sections were then treated with citric acid to facilitate antigen retrieval, followed by three washes in PBS. Samples were next blocked for

1 h using serum, followed by probing overnight at 4°C with appropriate primary antibodies, further washing, and probing for 1 h at room temperature using fluorescently conjugated secondary antibodies. Samples were then imaged via Olympus FV300 confocal microscope (200×). To ensure accuracy, 4-5 fields of view in different cortical regions were selected at random, with positive areas being averaged across these regions.

Western blotting

The expression of Sphk1 (NOVUS Biologicals, JA31-14), MAPLC3 II (Cell Signaling Technology, D11), SQSTM1/p62 (Abcam, ab155686) and TRAF2 (Abcam, ab126758) in OGDR and MCAO model systems was measured via Western blotting. Briefly, protein levels in ischemic penumbra tissue samples were quantified via BCA assay. Next, 10-12% SDS-PAGE was used to separate the proteins, and they were transferred onto cellulose acetate membranes. Blots were next blocked for 2 h using 5% non-fat milk followed by overnight probing with primary antibodies at 4°C. Blots were then washed prior to probing for 1 h with appropriate fluorescent secondary antibodies. Blots were then imaged with an infrared Odyssey 3.0 instrument, with β-actin being used as a means of normalizing protein expression across samples.

Lentiviral knockdown of SphK1

SphK1-knockdown rats were generated via administering 3.5% chloral hydrate (350 mg/kg) to anesthetize rats and placing them within a stereotactic device. A lentivirus targeting SphK1 (GenePharma Corporation Shanghai, China) was then directly administered (2 μg/μl) to the right lateral ventricle at a position 1.0 mm behind the anterior iliac crest, 2.0 mm to the side of the stereotactic instrument using the midline for guidance, and 3.5 mm ventral of the surface of the skull. At 2 weeks post-injection, rats were subjected to MCAO procedures.

Injection of inhibitors

Selected inhibitory compounds (RAP and 3-MA, Sigma) were administered at doses selected based upon prior studies (23-25). RAP and 3-MA were both delivered via intracerebroventricular injection (i.c.v.). Dosing with RAP (35 pmol; dissolved in ethanol and diluted to < 2% ethanol using normal saline) was conducted at both 2 h prior to MCAO and 24 h post-perfusion, while 3-MA was administered at the onset of reperfusion.

Culture of primary cells

Neonatal rats (1-2 days old) were used as a source for primary microglia. Briefly, animals were euthanized and the meninges and cortical tissue were separated from one another. The cortices were then dissociated and passed through a 200 μm filter. The filtered cells were resuspended in high glucose (4.5 g/L) DMEM containing 5% fetal calf serum and penicillin/streptomycin (all from Hyclone, USA). Cells were then cultured at 37 °C. On day 10 of this culture process, flasks were shaken overnight (300 rpm) at 37 °C, and purified microglia were collected and cultured for 2-3 days in media prepared as above (complete media) with the addition of 1% microglia growth supplement (ScienCell, USA).

Immunocytochemical staining for the microglial marker Iba1 was used to confirm that these cultures were at least 98% pure.

To culture primary neurons, SD rats (embryonic day 17) were utilized as in previous reports (26). First, meninges were removed and cortical tissue was dissected, with the resulting tissue fragments being used to prepare a single cell suspension via passage through a 200 μm filter. The resultant cells were then cultured for 7-9 days using Neurobasal ™ medium supplemented with 2% B27 supplement (both from Invitrogen) and penicillin/streptomycin, after which cells were used for downstream experiments. Cultures were confirmed to be at least 96% pure based on staining for NeuN.

Lentiviral infection

Lentiviruses carrying an SphK1-specific shRNA (Lv-SphK1-shRNA) were prepared using the AdEasy lentivirus Vector System (GenePharma, Shanghai, China) via cloning the appropriate sequence into the pShuttle-CMV vector, followed by subsequent recombination into the pAdeasy-1 lentiviral vector. The resultant lentivirus was used to infect microglia for 24 h at a high titer (MOI = 100). Media was then exchanged for fresh complete media with appropriate supplements and the cells were cultured for 24 h, after which they were again infected as above.

OGDR treatment

Cells were used for *in vitro* OGDR modeling experiments. OGDR conditions were achieved by removing normal cellular media and instead culturing cells for 2 h in Earle's balanced salt solution (with no added glucose) at 37°C in a low-oxygen (95% N_2/3% CO_2/2%O_2) incubator. In parallel, control cells were cultured in Earle's balanced salt solution containing 10 mM glucose in a normoxic incubator. After the 2 h low-oxygen incubation, cells were then returned to a normoxic incubator as a means of initiating reperfusion.

Electron microscopy

Phosphate-buffered glutaraldehyde (2.5%) and osmium tetroxide (1%) were used to fix samples, after which they were dehydrated using a series of graded acetone solutions. Epoxy resin was then used to embed tissues, after which semi-thin (1 mm) tissue sections were prepared and toluidine blue-stained. Sections that were 600-Å thick were then prepared from these stained sections, with the resultant sections being lead citrate and uranyl acetate stained. A transmission electron microscope (JEM-1200X, SHIMADZU, Japan) was then used to visualize 5-8 random fields of view per brain section (13,500 ×; n=6 rats/group).

Cellular transfection

In order to knock down TRAF2 expression, microglia cultured as above were transfected with either a negative control siRNA or a rat TRAF2-specific siRNA at 70 nM with the XtremeGENE siRNA transfection reagent (Roche) based on provided directions. Briefly, cells were plated in 12-well plates at 1.4×10^5/well, and were allowed to rest for 48 h post-transfection prior to downstream use. A pEGFP expression vector

(BD Biosciences Clontech, CA, USA) was used in parallel wells as a means of monitoring the efficiency of transfection, which was usually > 70%.

Measurement of apoptotic cell death

The survival of OGDR-treated cells was analyzed using a TUNEL staining kit (Roche, Switzerland). Briefly, neurons that had been cultured on coverslips were fixed using 4% paraformaldehyde, after which they were treated using 0.3% hydrogen peroxide to quench any endogenous peroxidase activity. Samples were then incubated for 1 h with the TUNEL reaction solution, followed by a 30 minute counterstain with DAPI at 37 °C. After staining, cell samples were assessed via fluorescent microscopy (Olympus), with the TUNEL staining frequency being determined by normalizing TUNEL-positive areas in individuals to total DAPI-positive area.

ELISAs

OGDR-induced production of IL-1β, IL-6, and TNF-α by microglia was quantified in cell culture supernatants at the indicated time points via ELISA based on provided directions. Briefly, 96-well plates were initially coated overnight with capture antibodies specific for these cytokines of interest (2–4 μg/ml). Next, 1% BSA was used to block these plates, after which 50 μl of appropriate standards or samples were added to each well. Plates were then washed and probed with a biotinylated secondary antibody, followed by further washing and streptavidin-mediated color development. Absorbance at 450 nm was then measured to quantify protein levels.

Detection of apoptosis by flow cytometry

Primary neurons were seeded in 6-well plates at a density of 5 × 105 cells/well. After 7 days, they were transduced with an appropriate lentivirus, and were then subjected to hypoxic conditions. Cells were then collected, washed with PBS, and 1x105 cells were resuspended in 500 μL of binding buffer. Cells were then stained using an Annexin-V-Fluos kit based on provided directions, with 100 μL of reaction solution being added per sample containing HEPES, Annexin-V, and PI. After staining for 15 minutes, 1 mL of PBS was added per sample, and cells were then analyzed via flow cytometry.

Statistical analysis

Data are presented as means ± standard deviation from triplicate experiments. Data were compared via Student's t-tests and ANOVAs as appropriate using SPSS v22.0. $P < 0.05$ was the significance threshold for these analyses.

Results

Analysis of autophagy-related protein levels in microglia in response to cerebral I/R

In previous analyses of murine focal cerebral ischemia model systems, ischemia has been shown to induce microglial autophagy, inflammation, and neuronal damage (21). We began our study be monitoring autophagic activity in rat brain peri-infarct cortical microglia at 12, 24, and 48 h post-cerebral I/R. To monitor autophagic activity, we assessed the levels of both MAP1LC3 and SQSTM1/p62, with the former being an autophagy marker that is converted from a soluble form (MAP1LC3-I) to a lipidated form (MAP1LC3-II) during autophagy, and the latter being an autophagic cargo protein used to monitor autophagic flux (27). We observed increasing microglial MAP1LC3 levels in ischemic cortical tissue following cerebral I/R, with peak expression after 24 hours (10.5 ± 0.25), and with a gradual decrease at 48 h (Fig. 1A, B), whereas SQSTM expression was lowest at 24 hours (5.5 ± 0.3) (Fig. 1C, D). These findings were consistent with cerebral I/R having induced autophagy within microglia, with peak induction occurring after 24 h.

Inhibition of SphK1 is sufficient to suppress cerebral I/R-induced microglial autophagy

We have previously demonstrated that maximal SphK1 expression in microglia occurs at 24 h post-cerebral I/R or -OGDR (11). To explore the physiological importance of SphK1 in our model system, we introduced a lentivirus targeting SphK1 into the lateral ventricle of rats in order to inhibit this enzyme prior to utilizing MCAO as a means of modeling cerebral I/R. We observed significantly lower SphK1 expression (7.5 ± 0.3) in Lv-Sphk1 infected rats in peri-infarct cortical tissue in vivo at 24 h post-cerebral I/R (Fig. 2A, B). This inhibition also coincided with both reduced MAP1LC3 expression (6.0 ± 0.3) and increased SQSTM1 expression (7.0 ± 0.3) in these rats at the same time point (Fig. 2C-F). SphK1 inhibition was also associated with a reduction in autophagosome numbers (1.75 ± 0.15), as confirmed via electron microscopic visualization of dual-membrane-enclosed vacuolar structures within these cells at 24 h post-cerebral I/R (Fig. 2G, H). Together, these findings therefore suggest that SphK1 is directly responsible for mediating autophagic induction within microglia in response to cerebral I/R.

Inhibition of SphK1 reduces cerebral I/R-induced apoptotic neuronal death via suppressing autophagy

A dominant-negative form of Sphk1 inhibits autophagosome synthesis in neurons, suggesting that Sphk1 plays a role in the biogenesis of autophagosomes (28). In the present study, we evaluated whether SphK1 could also induce autophagy in neurons in response to cerebral I/R. As shown in Fig. 3A-B, the number of SphK1 positive neurons decreased significantly after SphK1 knockdown. Moreover, SphK1 knockdown decreased MAP1LC3 expression on neurons (Fig. 3C, D). Inhibition of microglial SphK1 has been shown to inhibit the production of proinflammatory cytokines and the apoptotic death of neurons in the context of cerebral I/R (11, 26, 29). We also observed significantly more TUNEL-positive apoptotic neurons in rats at 24 h post-cerebral I/R relative to numbers in Sh-SphK1-treated animals at this same time point (19.5%±0.4). When the autophagy activator RAP was injected into the lateral ventricle of these rats, we observed a further reduction in TUNEL-positive cell frequencies (11%±0.3), whereas the autophagic inhibitor 3-MA significantly increased this frequency (29%±2) (Fig. 3E, F). Together, these findings suggest that SphK1 is at least partially responsible for neuronal apoptosis in the context of cerebral I/R, functioning via an autophagy-dependent mechanism.

OGDR drives microglial SphK1 upregulation and autophagy *in vitro*

Previous work has clearly emphasized the fact that cerebral hypoperfusion and ischemia can result in microglial activation, autophagy, and inflammation (20, 21). In order to gain further mechanistic insights into the relationship between cerebral I/R and SphK1 expression in our model system, we utilized purified microglia in an *in vitro* OGDR model as a means of mimicking the effect of cerebral I/R on autophagy in these cells. We found that OGDR resulted in an increase in SphK1 (11 ± 0.15) and LC3II (9 ± 0.28) expression after 24 h, whereas SQSTM1 levels were reduced at this same time point (0.5 ± 0.1) (Fig. 4A-D). Much as was observed *in vivo*, we detected SphK1 and MAP1LC3II in the cytosol of these microglia at 24 h post-OGDR, with reduced SQSTM1 levels also being observed at this time point (Fig. 4E). This, therefore, suggested that OGDR can directly induce SphK1 upregulation and autophagy within microglia after 24 h.

SphK1 knockdown inhibits OGDR-induced autophagy and thereby protects against neuronal apoptosis

We next explored the mechanistic importance of SphK1 in the OGDR-mediated induction of microglial autophagy and neuronal damage. To that end, we knocked down SphK1 in microglial cells using a specific lentiviral construct. After a 48 h rest, we subjected these cells to OGDR modeling. We found that SphK1 knockdown was associated with both significantly reduced MAP1LC3II expression (0.65 ± 0.2) and markedly elevated SQSTM1 expression (1.4 ± 0.2) (Fig. 5A, B). Cells in which SphK1 had been knocked down also exhibited fewer autophagosomes when assessed via electron microscopy (Fig. 5C). Intracellular S1P has also been reported to drive pro-inflammatory signaling, although anti-inflammatory S1P-mediated chemokine suppression has also been documented (30). We evaluated the effect of SphK1 inhibition on S1P, and found that S1P levels in microglial supernatants decreased after SphK1 inhibition (Fig. 5D). When we exposed neurons cultured under OGD conditions to supernatants from OGDR-activated microglia, we observed significantly lower rates of neuronal apoptosis when supernatants were derived from SphK1-knockdown cells (4.1 ± 0.3%) than when they were derived from control cells (10.2 ± 0.18%). Treatment of cells with RAP to activate autophagy further enhanced the apoptotic death of OGD neurons (7.2 ± 0.2%) (Fig. 5E, F). These decreases in neuronal apoptosis also coincided with flow cytometry results (6.25%±0.15%) (Fig. 5G, H). Together, these findings confirmed the importance of microglial SphK1 as a mediator of both microglia-intrinsic autophagy and microglia-induced neuronal apoptosis in this OGDR model system.

Inhibiting microglial autophagy is sufficient to reduce OGDR-associated neuronal damage

We further investigated the mechanistic role of microglial autophagy in the induction of neuronal cell death in our OGDR system. To that end, we subjected microglia to OGDR conditions for 24 h, after which 3-MA (10 mmol/L) or RAP (200 nmol/L) were added to the culture media at the time of reoxygenation. We found that 3-MA-mediated inhibition of autophagy was sufficient to reduce the production of the pro-inflammatory cytokines IL-1β, IL-6, and TNF-α by these cells, whereas the opposite phenotype was observed when cells were instead treated with RAP to activate autophagy (Fig. 6A). We then exposed OGD-treated neurons to the supernatants from 3-MA- or RAP-treated microglia, revealing that

supernatants from 3-MA-treated cells were associated with significantly lower levels of apoptosis (5.4 ± 0.2% loss) as compared to control supernatants (12.1 ± 0.3% loss), whereas RAP-treated microglial supernatants were associated with a slightly lower rate of observed neuronal apoptosis (8.5 ± 0.28% loss) (Fig. 6B, C). Flow cytometry findings were consistent with TUNEL staining results (Fig. 6D, E). These findings thus strongly suggested that the induction of microglial autophagy under OGDR conditions is sufficient to aggravate OGDR-associated neuronal damage.

SphK1 promotes OGDR-induced autophagy and neuronal injury via TRAF2 in microglia

Previous work has shown that SphK1 can be activated in response to TNF, whereupon it phosphorylates sphingosine to generate S1P, which subsequently interacts with the downstream signaling factor TRAF2 (31). Sphk1 can stimulate autophagy through TRAF2 (18). As such, we hypothesized that SphK1 may regulate autophagy in our model system in a TRAF2-dependent fashion. Consistent with this, we found that siRNA-mediated knockdown of TRAF2 was sufficient to reduce MAP1LC3-II expression and to increase SQSTM1 levels following SphK1 knockdown in OGDR-treated microglia after 24 h. (Fig. 7. A-C). When supernatants from these cells were then used to treat OGD-exposed neurons, we similarly found that SphK1 knockdown-induced neuronal apoptosis was inhibited following TRAF2 silencing (3.5 ± 0.2% loss) (Fig. 7D). Flow cytometry results were consistent with TUNEL staining findings (Fig. 7E, F), thus suggesting that SphK1 is able to drive the OGDR-mediated induction of autophagy in microglial via a pathway dependent upon TRAF2.

Discussion

SphK family enzymes, which are essential for the generation of S1P from sphingosine, play key roles in intracellular signaling and in the coordination of inflammatory responses (32). In macrophages, the inhibition of SphK activity has been shown to not only enhance intracellular sphingolipid levels, but also to alter intracellular autophagic activity (33). In the present study, we first confirmed that cerebral I/R was sufficient to induce the upregulation of SphK1 and LC3 II as well as the downregulation of SQSTM1, all of which are markers of autophagy (Fig. 1). When SphK1 was knocked down using a lentiviral vector, this impaired autophagic induction in microglia and also protected proximal neurons from apoptotic death (Fig. 2). SphK1 can also be expressed in neurons, astrocytes, and cerebellar granule cells. In our experiment, the presence of Iba1-negative SphK1 in brain tissue was observed in the context of cerebral ischemia-reperfusion (Fig. 2 white arrows), and prior work has shown that Sphk1 regulates autophagy in neurons (28, 34). In this case, lentivirally pretreated rat brain tissue samples yielded evidence of SphK1-mediated neuronal apoptosis, autophagy, and ultimately death (Fig. 3). Together, our findings strongly indicate that SphK1- induced autophagy within microglia can drive neuronal injury in response to cerebral I/R.

TRAF2, an established downstream component of the SphK1 intracellular signaling pathway, regulates a variety of cellular activities and thereby facilitates the lysine 63-linked ubiquitination of signaling proteins such as RIPK1 and TICAM1 (31, 35). Sphk1 promotes EMT via stimulating the TRAF2-mediated lysine 63-

linked direct ubiquitination of BECN1 through the intracellular S1P-stimulated pathway, inducing the lysosomal degradation of CDH1 in HepG2 cells (18, 35, 36). However, other researchers (33, 37) have found that TRAF2, but neither SphK1 nor SphK2, are required for the TNF-mediated activation of NF-κB and MAP kinase signaling. In our study, we determined that SphK1-induced autophagy in microglia was at least partially dependent upon TRAF2 in an I/R model system (Fig. 7). Therefore, we speculate that the relationship between TRAF2 and SphK1 in this context is distinct from the mechanisms described above, although further research is needed to confirm this hypothesis.

Many studies have clearly highlighted a role for autophagy in the pathogenesis of CIRI, with neuron survival being closely linked to autophagic activity (38, 39). Specifically, hypoxia- and ischemia-induced autophagy has been shown to protect neurons from death in the context of CIRI. Treatment with rapamycin can further induce autophagy, thereby providing additional protection against neuronal death and associated brain injury (40). In contrast, however, other studies have suggested that autophagy can drive neuronal death in a rat MCAO model system wherein excessive autophagy can aggravate brain damage (41). In this model, the use of 3-MA to inhibit autophagy reduces neuronal apoptosis in treated animals (42). In the present study, we determined that autophagic induction was associated with adverse outcomes (Fig. 1, Fig. 4), whereas inhibiting autophagy reduced microglia-induced nerve damage (Fig. 5).

S1P is a critical mediator of immune functionality and is implicated in a range of autoimmune diseases, inflammatory and metabolic disorders, and infections (6, 43) have shown that the S1P-S1PR2 axis drives inflammation and autophagic defects. As such, the function of S1P signaling in the context of inflammation is complex and varies in a disease- and site-specific manner. In this study, we confirmed that the level of S1P decreased after SphK1 knockout, and that the impact of SphK1 inhibition on OGDR-induced autophagy may be related to S1P.

The extensive autophagic activity observed in activated microglia may be a compensatory mechanism induced to prevent the excessive activation of these cells as a means of maintaining homeostasis. Defective autophagy within these cells would potentially lead to the accumulation of defective organelles and proteins, thereby increasing ROS generation and consequent inflammation and apoptosis. This, therefore, suggests that the degree and timing of autophagic activation in microglia during cerebral I/R determine whether it is ultimately protective or deleterious. Further studies of the molecular mechanisms governing such determinations have the potential to highlight novel treatment avenues for IS patients.

Conclusion

In conclusion , our findings provide clear evidence that SphK1 facilitates CIRI-induced autophagy in microglia, in turn promoting inflammation and associated neuronal death. Therapeutic approaches targeting this signaling axis may therefore be of value for the treatment of cerebral ischemia.

Abbreviations

CIRI：cerebral ischemia-reperfusion injury；

OGDR: oxygen-glucose deprivation reperfusion；

IL-1β: Interleukin-1 beta;

IL-6: Interleukin-6;

IL17：interleukin-17；

NO: nitric oxide;

TNF-α: tumor necrosis factor；

ROS: reactive oxygen species；

TRAF2: tumor necrosis factor receptor-associated factor 2;

ELISA: enzyme-linked immunosorbent assay;

TUNEL: terminal transferase-mediated deoxyuridine triphosphate-biotin nick end labeling；

S1P: Sphingosine 1-phosphate;

SphK1：sphingosine kinase 1；

3-MA: 3-methyadenine；

MCAO: middle cerebral artery occlusion;

CCA: common carotid artery;

ECA: external carotid artery.

Declarations

Acknowledgements

Not applicable.

Authors' contributions

Manhua Lv designed and performed the experiments, wrote the manuscript. Yongjia Jiang and Yuanyuan Zeng performed the focal cerebral ischemia-reperfusion model, immunoassays and the western blotting analysis. Dayong Zhang helped with data collection and interpretation and contributed to critical manuscript revision. Dan Yao carried out the cell cultures. Wei Zhang and Yuefeng Cheng peformed detection of neuronal apoptosis. All authors read and approved the final manuscript.

Funding

This study was supported from the National Natural Science Foundation of China (Grant Nos. 81801185) and Foundation of Heilongjiang health and Family Planning Commission. (Grant Nos. 2017-034)

Availability of data and materials

The datasets supporting the conclusions of this article are included within the article.

Ethics approval

All procedures were strictly performed in accordance with the regulations of the ethics committee of the International Association for the Study of Pain and the Guide for the Care and Use of Laboratory Animals. All animal studies were approved by the School of Medical Science of Harbin Medical University, with all efforts having been made to reduce animal use and suffering when possible.

Consent for publication

Not applicable.

Competing interests

The authors declare that they have no competing interests.

References

1. Kim Y, Davidson JO, Green CR, Nicholson LFB, O'Carroll SJ, Zhang J.Connexins and Pannexins in cerebral ischemia. Biochim Biophys ActaJan 2018; 1860(1): 224-236.
2. Kim, J.Y., Jeong, H.Y., Lee, H.K., Kim, S., Hwang, B.Y., Bae, K., Seong, Y.H. Neuroprotection of the leaf and stem of Vitis amurensis and their active compounds against ischemic brain damage in rats and excitotoxicity in cultured neurons. Phytomedicine. 2012; Jan 15, 19(2), 150-9.
3. McDonough A, Weinstein JR. Neuroimmune Response in Ischemic Preconditioning. Neurotherapeutics. 2016; 13(4): 748-761.
4. Chen S, Dong Z, Cheng M, Zhao Y, Wang M, Sai N, Wang X, Liu H, Huang G, Zhang, X. Homocysteine exaggerates microglia activation and neuroinflammation through microglia localized STAT3 overactivation following ischemic stroke. J Neuroinflammation. 2017; 14(1): 187.
5. Edmonds Y, Milstien S, Spiegel S. Development of small-molecule inhibitors of sphingosine-1-phosphate signaling. Pharmacol Ther. 2011; 132, 352–60.
6. Spiegel S, Milstien S. The outs and the ins of sphingosine-1- phosphate in immunity. Nat. Rev. Immunol. 2011; 11, 403–15.
7. Hofmann LP, Ren S, Schwalm S, Pfeilschifter J, Huwiler A. Sphingosine kinase 1and 2 regulate the capacity of mesangial cells to resist apoptotic stimuli in an opposing manner. Biol Chem. 2008; 389:

1399–1407.

8. Neubauer HA, Pitson SM. Roles, Regulation and inhibitors of sphingosine kinase 2. FEBS J. 2013; 280: 5317–5336.
9. Shida D, Takabe K, Kapitonov D, Milstien S, Spiegel, S. Targeting SphK1 as a newstrategy against cancer. Curr. Drug. Targets. 2008; 9, 662–673.
10. Zheng S, Wei S, Wang X, Xu Y, Xiao Y, Liu H, Jia J, Cheng J. Sphingosine kinase 1 mediates neuroinflammation following cerebral ischemia. Exp Neurol. 2015; 272: 160–169.
11. Lv M, Zhang D, Dai D, Zhang W, Zhan, L. Sphingosine kinase 1/sphingosine-1-phosphate regulates the expression of interleukin-17A in activated microglia in cerebral ischemia/reperfusion. Inflamm Res 2016; 65(7): 551-562.
12. Lavieu G, Scarlatti F, Sala G, Carpentier S, Levade T, Ghidoni R, Botti J, Codogno P. Regulation of autophagy by sphingosine kinase 1 and its rolein cell survival during nutrient starvation. J Biol Chem. 2006; 281: 8518-27.
13. Maceyka M, Harikumar KB, Milstien S, Spiegel S. Sphingosine-1-phosphate signaling and its role in disease. Trends Cell Biol. 2012; 22: 50-60.
14. Lavieu G, Scarlatti F, Sala G, Carpentier S, Levade T, Ghidoni R, Botti J, Codogno P. Sphingolipids in macroautophagy. Methods Mol Biol. 2008; 445: 159-73.
15. Vallabhapurapu S, Matsuzawa A, Zhang W, Tseng PH, Keats J J, Wang H, Vignali DA, Bergsagel PL, Karin M.Nonredundant and complementary functions of TRAF2 and TRAF3 in a ubiquitination cascade that activates NIK-dependent alternative NF-κB signaling. Nat Immuno. 2008 Dec;9(12):1364-70.
16. Devin A, Lin Y, Yamaoka S, Li Z, Karin M, Liu Z. The α and β subunits of IκB kinase (IKK) mediate TRAF2-dependent IKK recruitment to tumor necrosis factor (TNF) receptor 1 in response to TNF. Mol Cell Biol. 2001; 21: 3986–3994.
17. Liu SF, Malik AB. NF-κB activation as a pathological mechanism of septic shock and inflammation. Am J Physiol Lung Cell Mol Physiol. 2006; 290: L622–645.
18. Liu H, Ma Y, He H, Zhao WL, Shao RG. SPHK1 (sphingosine kinase 1) induces epithelial-mesenchymal transition by promoting the autophagy-linked lysosomal degradation of CDH1/E-cadherin in hepatoma cells. Autophagy. 2017 May 4;13(5):900-913.
19. Su P，Zhang J，Wang D，Zhao F, Cao Z, Aschner M, Luo W. The role of autophagy in modulation of neuroinflammation in microglia. Neuroscience. 2016; 319: 155-167.
20. Yang Z，Zhang N，Shen H，Lin C, Lin L, Yuan B. Microglial activation with reduction in autophagy limits white matter lesionsand improves cognitive defects during cerebral hypoperfusion. Curr Neurovasc Res 2014; 11(3): 223-229，
21. Yang Z, Zhong L, Zhong S, Xian R, Yuan B. Hypoxia induces microglia autophagy and neural inflammation injury in focalcerebral ischemia model. Exp Mol Pathol. 2015; 98(2): 219-224.

22. Yin S, Miao Z, Tan Y, Wang P, Xu X, Zhang C, Hou W, Huang J, Xu H. SPHK1-induced autophagy in peritoneal mesothelial cell enhances gastric cancer peritoneal dissemination. Cancer Med. 2019; 8(4): 1731-1743.
23. Sheng R, Zhang LS, Han R, Liu XQ, Gao B, Qin ZH. Autophagy activation is associated with neuroprotection in a rat model of focal cerebral ischemic preconditioning. Autophagy. 2010; 6: 482–494.
24. Qin AP, Liu CF, Qin YY, Hong LZ, Xu M, YangL, Liu J, Qin Z, Zhang Autophagy was activated in injured astrocytes and mildly decreased cell survival followingglucose and oxygen deprivation and focal cerebral ischemia. Autophagy. 2010;6: 738–753.
25. Gao L, Jiang T, Guo J, Liu Y, Cui G, Gu L, SuL, Zhang Inhibition of autophagycontributes to ischemic postconditioning-induced neuroprotection against focalcerebral ischemia in rats. PLoS One. 2012; 7: e46092
26. Su D, Cheng Y, Li S, Dai D, Zhang W, Lv M. Sphk1 mediates neuroinflammation and neuronal injury via TRAF2/NF-kappaB pathways in activated microglia in cerebral ischemia reperfusion. J Neuroimmunol 2017; 305: 35-41.
27. Liu H, Ma Y, He HW, Wang JP, Jiang JD, Shao RG. SLC9A3R1 stimulates autophagy via BECN1 stabilization in breast cancer cells. Autophagy 2015; 11: 232
28. Moruno Manchon JF, Uzor NE, Dabaghian Y, Furr-Stimming EE, Finkbeiner S, Tsvetkov AS.Moruno Manchon JF, et al. Cytoplasmic sphingosine-1-phosphate pathway modulates neuronal autophagy. Sci Rep. 2015 Oct 19;5:15213.
29. Onder, T.T., Gupta, P.B., Mani, S.A., Yang, J., Lander, E.S., Weinberg, R.A. Loss of E-cadherin promotes metastasis via multiple downstream transcriptional pathways. Cancer. Res. 2008; 68, 3645-54
30. Adada M, Canals D, Hannun YA, Obeid LM. Sphingosine-1-phosphate Receptor 2. FEBS J. 2013; 280(24): 6354-66.
31. Alvarez SE, Harikumar KB, Hait NC, Allegood J, Strub GM, Kim EY, Maceyka M, Jiang H, Luo C, Kordula T, Milstien S, Spiegel S. Sphingosine-1-phosphate is a missing cofactor for the E3 ubiquitin ligase TRAF2. Nature. 2010; 465:1084–1088.
32. Liu H, Sugiura M, Nava V E, Edsall L C, Kono K, Poulton S, Milstien S, Kohama T, Spiegel S. Molecular cloning and functional characterization of a novel mammalian sphingosine kinase type 2 isoform. J Biol Chem. 2000; 275: 19513–19520.
33. Xiong Y, Lee HJ, Mariko B, Lu YC, Dannenberg AJ, Haka AS, Maxfield FR, Camerer E, Proia RL, Hla T. Sphingosine kinases are not required for inflammatory responses in macrophages. J Biol Chem .2013; 20, 291(21): 11465.
34. Moruno Manchon JF, Uzor NE, Finkbeiner S, Tsvetkov AS.Moruno Manchon JF, et al. SPHK1/sphingosine kinase 1-mediated autophagy differs between neurons and SH-SY5Y neuroblastoma cells. 2016; Aug 2;12(8):1418-24.
35. Sasai M, Tatematsu M, Oshiumi H, Funami K, Matsumoto M, Hatakeyama S, Seya T. Direct binding of TRAF2 and TRAF6 to TICAM- 1/TRIF adaptor participates in activation of the Toll-like receptor 3/4

pathway. Mol Immuno 2010; 47: 1283-91;

36. Shi CS, Kehrl JH. TRAF6 and A20 regulate lysine 63-linked ubiquiti nation of Beclin-1 to control TLR4-induced autophagy. Sci Signal. 2010; 25, 3(123): ra42.
37. Etemadi N, Chopin M, Anderton H, Tanzer MC, Rickard JA, Abeysekera W, Hall C, Spall SK, Wang B, Xiong Y, Hla T, Pitson SM, Bonder CS, Wong WW, Ernst M, Smyth GK, Vaux DL, Nutt SL, Nachbur U, Silke J. TRAF2 regulates TNF and NF-κB signalling to suppress apoptosis and skin inflammation independently of Sphingosine kinase 1. 2015 Dec 23;4:e10592
38. Liu Y, Xue X, Zhang H, Che X, Luo J, Wang P, Xu J, Xing Z, Yuan L, Liu Y, Fu X, Su D, Sun S, Zhang H, Wu C, Yang J. Neuronal-targeted TFEB rescues dysfunction of the autophagy-lysosomal pathway and alleviates ischemic injury in permanent cerebral ischemia. Autophagy. 2019 Mar;15(3):493-509.
39. Wang P, Shao B Z, Deng Z, Chen S, Yue Z, Miao CY. Autophagy in ischemic stroke. Prog Neurobiol. 2018; 163-164: 98–117.
40. Carloni S, Girelli S, Scopa C, Buonocore G, Longini M, Balduini W. Activation of autophagy and Akt/CREB signaling play an equivalent role in the neuroprotective effect of rapamycin in neonatal hypoxia-ischemia. Autophagy. 2010; 6: 366–377.
41. Morselli E, Tasdemir E, Maiuri M C, Galluzzi L, Kepp O, Criollo A, Vicencio JM, Soussi T, Kroemer G. Mutant p53 protein localized in the cytoplasm inhibits autophagy. Cell Cycle. 2008; 7: 3056–3061.
42. Chen N, Debnath J. Autophagy and tumorigenesis. FEBS Lett. 2010; 584(7): 1427-35.
43. Karunakaran I, Alam S, Jayagopi S, Frohberger SJ, Hansen JN, Kuehlwein J, Hölbling BV, Schumak B, Hübner MP, Gräler MH, Halle A, van Echten-Deckert G. Neural sphingosine 1-phosphate accumulation activates microglia and links impaired autophagy and inflammation. Glia. 2019; 67(10): 1859-1872.

Figures

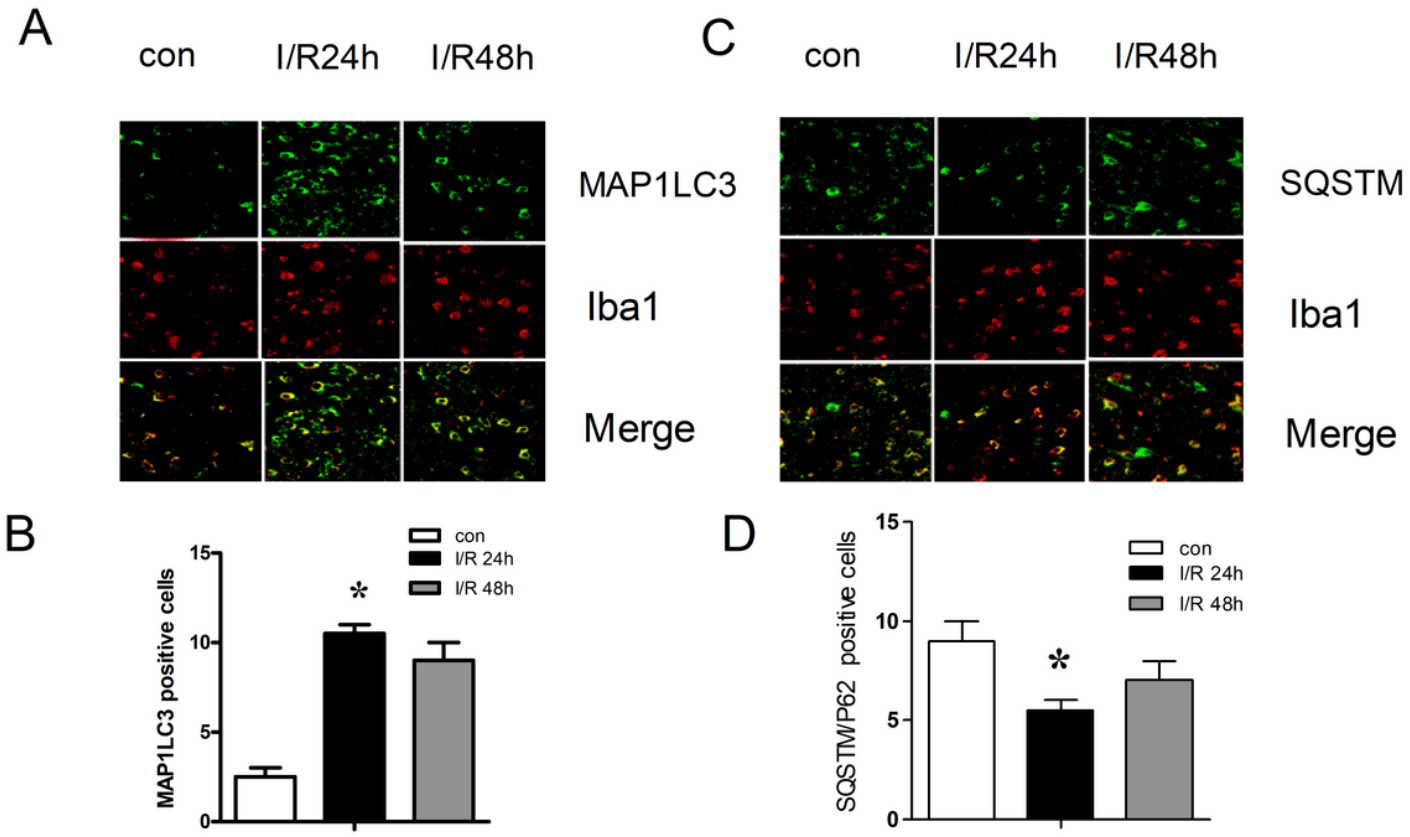

Figure 1

The expression of autophagy-associated proteins in a rat model of CIRI. (A, C) Sections of ischemic brain tissue were collected at 24 and 48 h post-CIRI modeling and were stained for LC3II, SQSTM1 (green), the microglial marker Iba1 (red), and nuclei counterstained with DAPI (blue). Samples were then imaged via confocal microscope. (B, D) LC3II/SQSTM1-positive cells were counted following CIRI. Data are means ± SD (n=5). *P<0.05 vs. control.

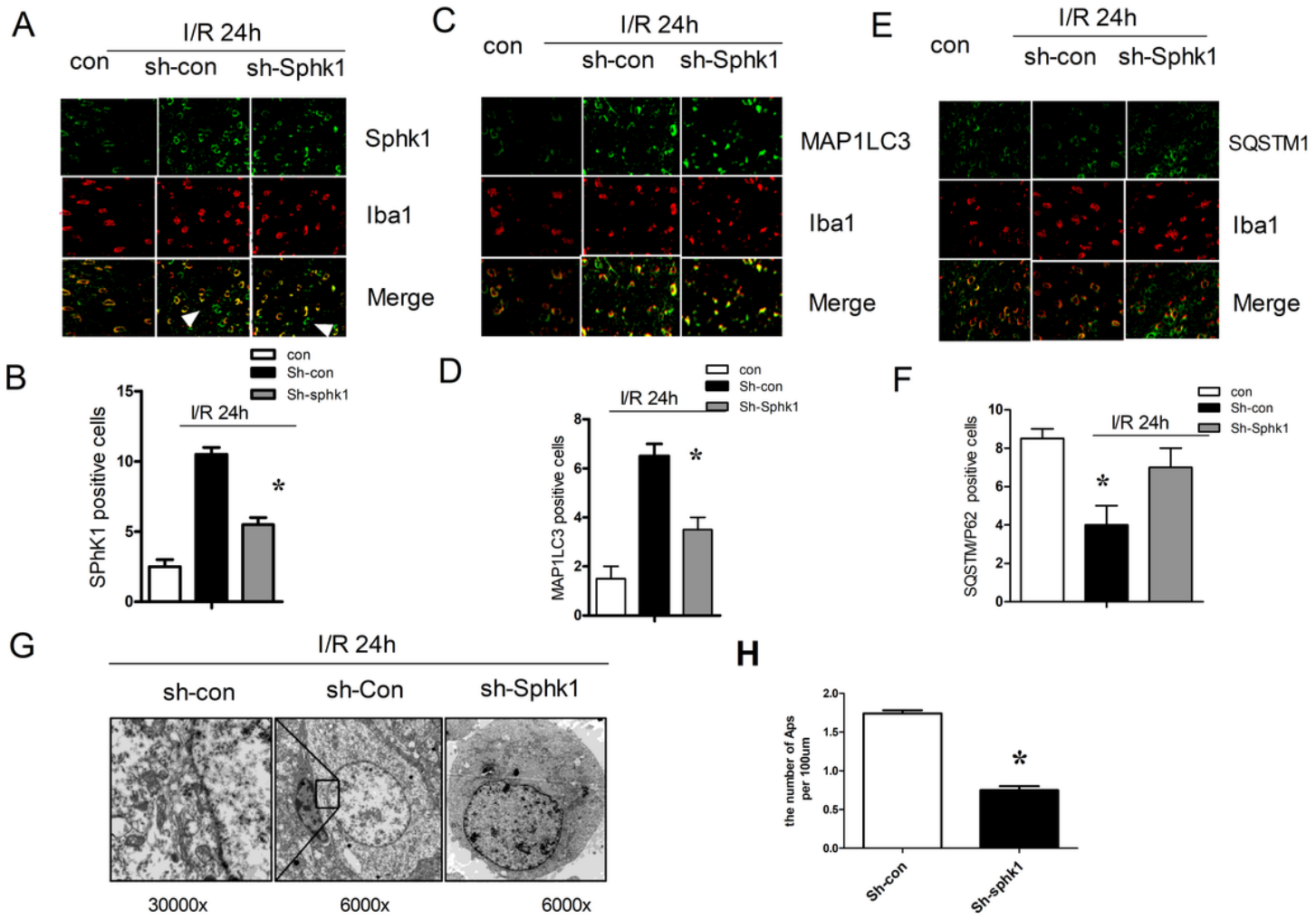

Figure 2

Lentiviral knockdown of SphK1 reduces microglial autophagy at 24 h in peri-infarct cortical tissue following CIRI. A lentivirus specific for SphK1 (2 μg/μl) was administered to the right ventricle of model rats two weeks prior to MCAO modeling. (A, C, E) Tissues were dual-stained for Sphk1/MAPLC3/SQSTM1 (green) and Iba1 (red) at 24 h post-CIRI, with DAPI (blue) used to counterstain nuclei. (B, D, F) The expression of SphK1/LC3II/SQSTM1 was quantified following CIRI. Data are means ± SD (n=5). *P<0.05 vs. control. (G, H) Representative autophagosomes were imaged at 24 h post-CIRI via electron microscopy (6000 - 30000 x).

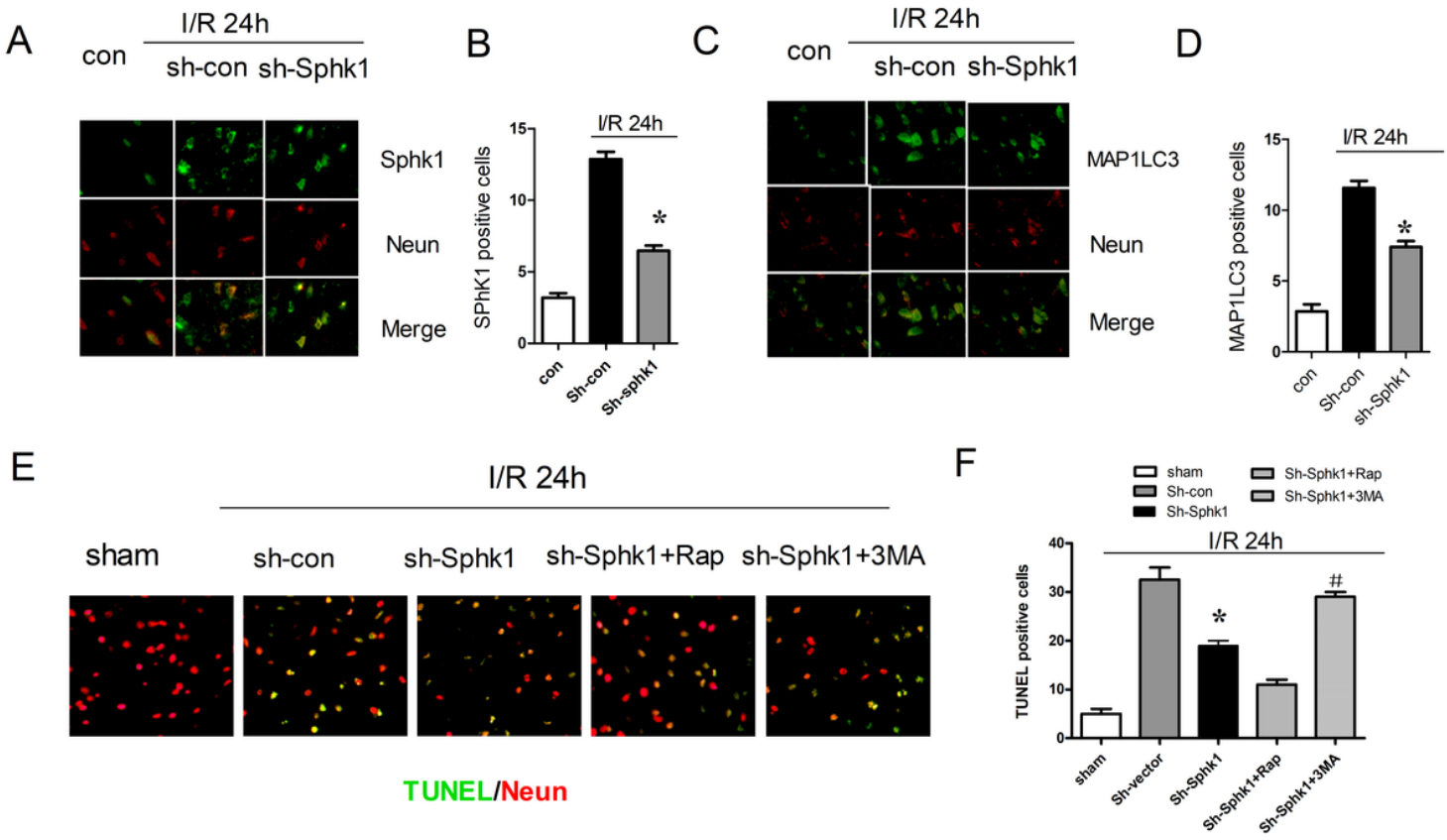

Figure 3

Knockdown of SphK1 suppresses autophagy and impairs neuronal apoptosis following CIRI. (A, C) A lentivirus specific for SphK1 (2 μg/μl) was administered to the right ventricle of model rats two weeks prior to MCAO modeling. Tissues were dual-stained for Sphk1/MAPLC3 (green) and Nenu (red) at 24 h post-CIRI, with DAPI (blue) used to counterstain nuclei. (B, D) The expression of SphK1/LC3II was quantified following CIRI. (E) Animals were administered 3-MA (i.c.v.). Alternatively, rapamycin (35 pmol, 5μl, i.c.v.) was administered both 2 h before MCAO and 24 h following reperfusion. TUNEL (green) and Neun (red) were used to stain neurons in cerebral tissue sections (200x). (F) The number of TUNEL-positive cells was quantified. Data are means±SD of at least three experiments.

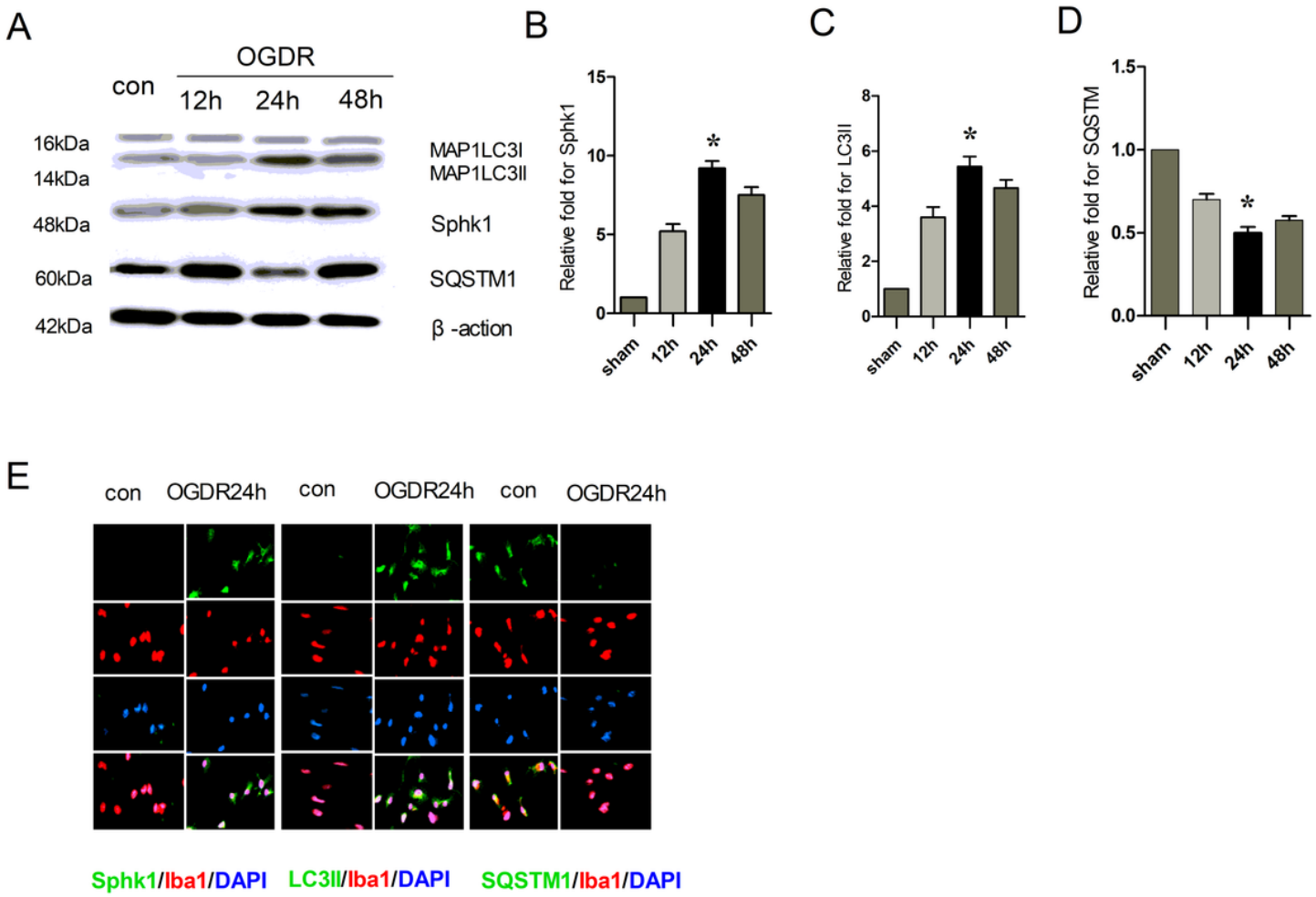

Figure 4

OGDR induces microglial SphK1 upregulation and autophagy in vitro. (A-D) Levels of SphK1, LC3II, and SQSTM in cultured microglia were measured at 12, 24, and 48 h post-OGDR, with β-actin used for normalization. (E) At 24 h post-OGDR, cells were fluorescently stained for Sphk1/LC3II/SQSTM (green) and Iba1/GFAP (red), with DAPI (blue) used for nuclear counterstaining prior to confocal microscopy. Data are means±SD of at least three experiments. *P<0.05 vs. control.

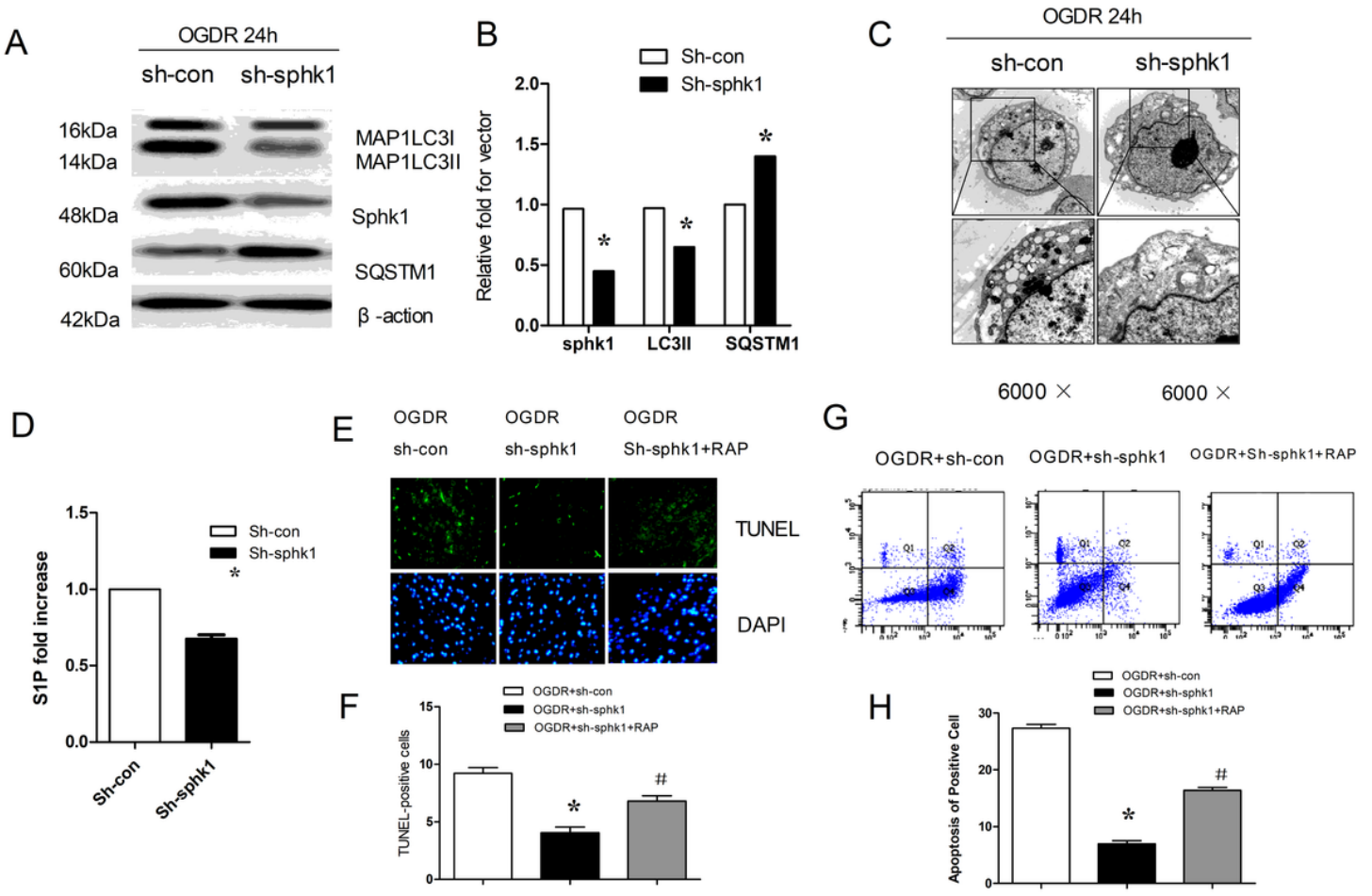

Figure 5

SphK1 knockdown in microglia reduces OGDR-induced autophagy and associated neuronal damage. (A, B) Levels of autophagy-related proteins in control or SphK1-specific lentivirus-treated microglia were quantified following OGDR via Western blotting. (C). Knockdown of SphK1 was associated with reduced autophagosome (AP) levels in microglia at 24 h post-OGDR. (D) Levels of S1P in microglial supernatants from cells treated as in (A) were quantified by ELISA. (E, F) OGD-exposed neurons were treated with supernatants from control or SphK1-knockdown microglia that were collected at 24 h post-OGDR. Cells were incubated for 24 h, followed by the analysis of neuronal apoptosis via TUNEL (green) and DAPI (blue) staining (200x). The percentage TUNEL-positive area (TUNEL/DAPI) was quantified. (G, H) The percentage of apoptotic neurons in each group was quantified by flow cytometry. Data are means±SD of at least three experiments. *P<0.05 vs. control. #P < 0.05.

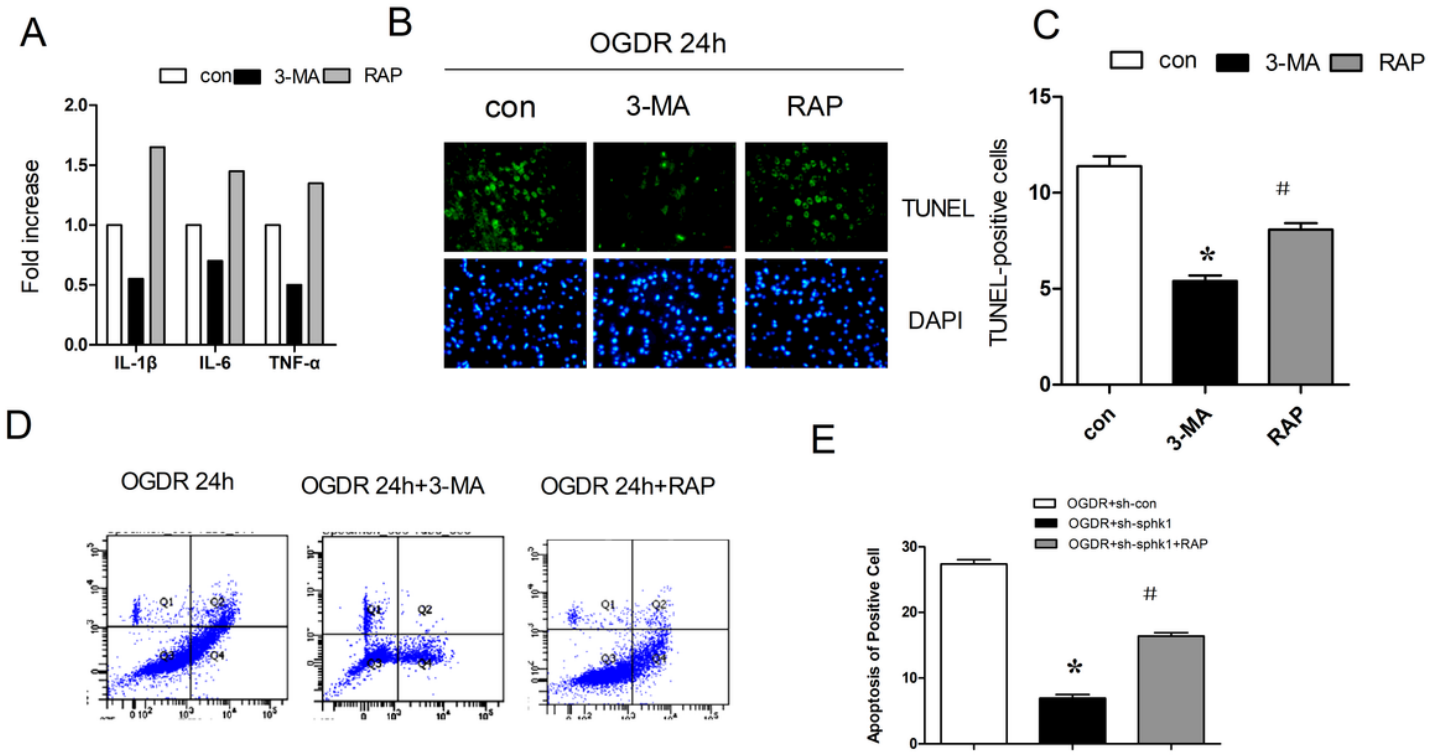

Figure 6

Inhibiting microglial autophagy reduced OGDR-induced neuronal damage. (A) Levels of IL-1β, IL-17, and TNF-α in microglial supernatants from cells treated via OGDR, ODGR+3MA, and OGDR+RAP were quantified by ELISA. (B) OGD-exposed neurons were treated with supernatants collected from microglia treated as in (A) at 24 h post-reperfusion. Neurons were cultured for 24 h, followed by the analysis of neuronal apoptosis via TUNEL (green) and DAPI (blue) staining (200x). (C, D) TUNEL-positive cells were quantified, and the percentage of TUNEL positive (TUNEL/DAPI) area was calculated. (E) The percentage of apoptotic neurons in each group was quantified by flow cytometry. Data are means±SD of at least three experiments. *P<0.05 vs. control. #P < 0.05.

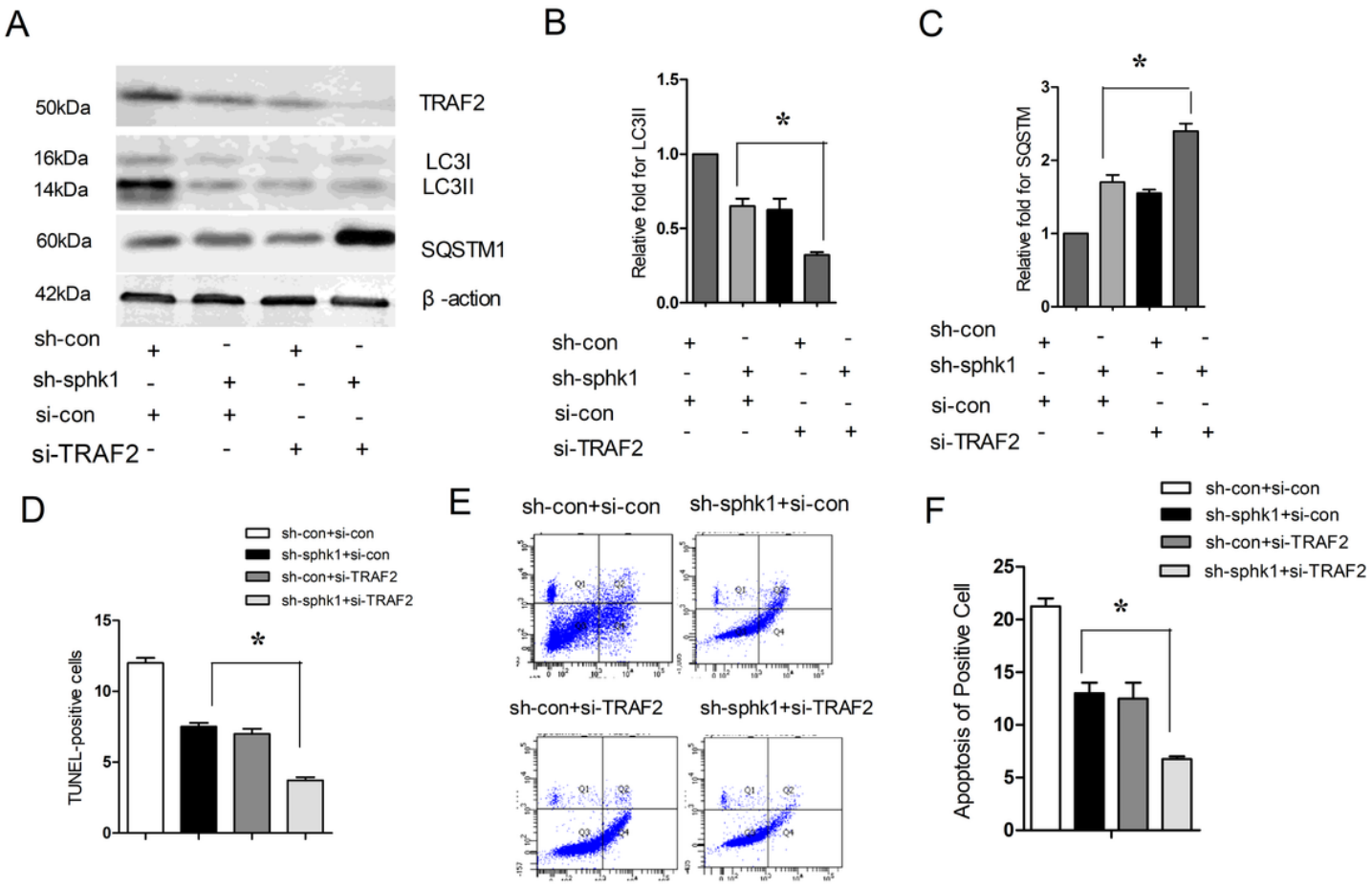

Figure 7

TRAF2 mediates SphK1-induced microglial autophagy and neuronal injury in response to OGDR conditions. (A-C) Knockdown of TRAF2 reduced LC3II levels in Sh-Sphk1 cells. Lysates were collected from these or control cells at 24 h post-OGDR 24h, after which Western blotting was used to quantify levels of autophagy-associated proteins. (D) OGD-exposed neurons were treated with microglial supernatants prepared in (A). Following a 24 h treatment, TUNEL-positive cells were quantified, and the percentage of TUNEL positive (TUNEL/DAPI) area was calculated. (E, F) The percentage of apoptotic neurons in each group was quantified by flow cytometry. Data are means±SD of at least three experiments.*P<0.05 vs. control.